

## THE EFFECT OF MAGNETITE PARTICLE SIZE ON PALEOINTENSITY DETERMINATIONS OF THE GEOMAGNETIC FIELD

SHAUL LEVI \*

*Geophysics Program, University of Washington, Seattle, Wash. 98195 (U.S.A.)*

(Revised and accepted for publication March 9, 1976)

Levi, S., 1977. The effect of magnetite particle size on paleointensity determinations of the geomagnetic field. *Phys. Earth Planet. Inter.*, 13: 245–259.

The Thellier method for paleointensity determinations has been applied to prepared samples containing magnetites whose mean particle sizes range from single domain, SD, to multidomain, MD. Linear (ideal) PNRM–PTRM curves are obtained for samples containing SD and submicron magnetite particles. However, for MD particles non-linear (concave-up) PNRM–PTRM curves are observed such that a linear approximation to the lower blocking-temperature data leads to apparent paleointensities that are higher than the actual paleo-field; however, the ratio of the end-points, NRM/TRM, yields the correct (laboratory) intensity. The non-linear (concave-up) PNRM–PTRM curves for the MD particles are explained in terms of the lack of symmetry of the domain-wall movements during the two heatings of the Thellier experiment. Low stabilities with respect to alternating fields and with respect to temperature cycles below magnetite's isotropic temperature are diagnostic in detecting samples most likely to exhibit non-linearities due to the MD effect.

### 1. Introduction

It is usually much more difficult to obtain a reliable estimate of the intensity of the earth's magnetic field from a certain rock or other remanence-bearing artifact than it is to obtain the direction of that field. Folgheraiter (1899) suggested the possibility of obtaining paleointensities from thermoremanent magnetization, TRM, of baked clays by comparing their original or natural remanence, NRM, which is assumed to be a pure TRM, with a laboratory TRM, obtained by heating the sample above its highest Curie temperature,  $T_C$ , and cooling it in the known laboratory field. Both the NRM and the laboratory TRM are assumed to be linearly proportional to the external field. A paleointensity estimate can then be obtained from the equation:

$$\frac{|J_n|}{|J_t|} = \frac{|h|}{|h_L|} \quad (1)$$

\* Currently at the Department of Geology and Geophysics, University of Minnesota, Minneapolis, Minn. 55455, U.S.A.

where  $J_t$  is the TRM produced in the laboratory in a field of strength  $h_L$ ;  $J_n$  is the measured NRM, and  $h$  is the unknown field intensity.

Physical and chemical changes are known to occur subsequent to the acquisition of the primary TRM, which may affect the intensity of the remanence, sometimes even in cases where the remanence direction remains unaltered. The probability that such a change has occurred during a rock's history increases with the rock's age, making reliable paleointensity determinations from older rocks very difficult.

In addition, it was recognized early (Folgheraiter, 1899) that one of the major sources of error in obtaining paleointensities is caused by chemical and physical alterations of the sample when it is heated in the laboratory. Indeed, Folgheraiter was discouraged from intensity studies because repeated TRM's were not self-consistent. The rate and extent of mineralogical and chemical reactions increase rapidly with temperature, and they may irreversibly affect the chemical and physical properties of the magnetic minerals and thus alter their TRM capacity and blocking tem-

peratures. Often, however, most of the physical and chemical changes occur upon the first heating to above  $T_C$ , such that internal consistency of subsequent TRM's might crown the result of the first laboratory TRM with false confidence. For these reasons it is imperative that any reliable method for paleointensity determinations have some sort of consistency checks to detect the presence and development of unwanted effects!

Since 1899, several methods for paleointensity determinations have been proposed (Thellier, 1938; Thellier and Thellier, 1959; Wilson, 1961; Van Zijl et al., 1962; Carmichael, 1967; Shaw, 1974). In principle, all these methods are similar in so far as they compare the NRM with a laboratory induced TRM, using specific bracketed segments of partial-NRM and partial-TRM to arrive at an estimate for the paleointensity. Each method has certain checks to assess whether the NRM is a pure TRM and whether the laboratory heating(s) alter(s) the sample's magnetic behaviour. Coe and Grommé (1973) compared three of the more common paleointensity methods in their study of historic lavas that erupted in known fields, and they find that the Thellier method yields the most reliable results. Therefore, this paper is limited to studying the Thellier method for paleointensity determinations.

The remanence of many continental igneous rocks resides in titanomagnetites with relatively low Ti content. For stoichiometric magnetite the upper size limit for single-domain, SD, particles is usually considered to be less than  $0.1 \mu\text{m}$  (see review by Evans, 1972; Butler and Banerjee, 1975). However, magnetic particles larger than  $1 \mu\text{m}$  are common in volcanic rocks and their fraction increases markedly in intrusive rocks. In addition, stable remanence, comparable to that of many igneous rocks, has been observed in natural and synthetic magnetite particles larger than the SD limit and also in particles larger than  $1 \mu\text{m}$  (Roquet, 1954; Morrish and Yu, 1955; Rimbart, 1959; Parry, 1965; Dunlop, 1973; Levi, 1974). The electron-microscope studies of Evans and Wayman (1970) suggest that the unusually stable remanence of the Modipe gabbro is carried by magnetite particles whose particle-size distribution peaks near  $0.25 \mu\text{m}$ . In addition, Soffel (1971) observed domain walls in titanomagnetite particles of composition  $(\text{Fe}_2\text{TiO}_4)_{0.55} \cdot (\text{Fe}_3\text{O}_4)_{0.45}$  with diameters as small as  $1.3 \mu\text{m}$ , suggesting that for Ti-free magnetite domain walls can exist in substantially

smaller grains. These results show that stable remanence resides in particles larger than SD; that is, in pseudosingle-domain, PSD, and multidomain, MD, particles. (PSD refers to particles whose sizes and magnetic properties are intermediate between those of "truly" SD and "truly" MD particles.)

It is often difficult to analyze a rock to determine the particular reason for the failure of a paleointensity determination, largely because rocks typically contain magnetic minerals that vary widely in their shapes, sizes, and sometimes compositions. This research was conducted in what appears to be the first well-controlled experiment where magnetic minerals of known compositions, sizes and shapes have been given a pure TRM in a known field and then subjected to a paleointensity method to determine whether or not a reliable estimate of the known field intensity can be extracted from that mineral. Magnetite ( $\text{Fe}_3\text{O}_4$ ) was chosen for this study for reasons of experimental convenience and because magnetite commonly occurs in continental rocks. Each sample was prepared to contain a narrow distribution of particle sizes and shapes, varying from SD to PSD to MD. The purpose of the study is to isolate the effects of particle size and domain state on the Thellier method for paleointensity determinations.

## 2. The Thellier method

The Thellier method for paleointensity determinations (Thellier and Thellier, 1959; Coe, 1967a,b) consists of a sequence of paired heatings to a given temperature  $T_1 < T_C$ . The two heatings are used to determine: (1) the partial-NRM (PNRM  $\equiv \Delta J_n$ ) that would be lost upon heating from room temperature,  $T_R$ , to  $T_1$  in zero field; and (2) the partial-TRM (PTRM  $\equiv \Delta J_t$ ) that would be acquired by cooling the sample in a known field,  $h_L$ , from  $T_1$  to  $T_R$ . Ideal behaviour in the Thellier sense is defined such that:

$$\frac{|\Delta J_n(T_2, T_1, h)|}{|\Delta J_t(T_2, T_1, h_L)|} = \frac{|h|}{|h_L|} \quad (2)$$

is obeyed for any temperature interval  $T_2, T_1$ . The notation  $\Delta J(T_2, T_1, h)$  refers to the magnetization acquired during cooling from  $T_2$  to  $T_1$  in a constant magnetic field,  $h$ . The subscripts n and t respectively

refer to NRM and TRM. In the Thellier method the temperature of the paired heatings is progressively increased from  $T_R$  until all blocking temperatures are exceeded, generating a data set  $[\Delta J_n(T), \Delta J_t(T)]$  for the different temperature steps. Each point gives an independent determination of  $|h|/|h_L|$ , providing the necessary self-consistency check. It is convenient to represent the data graphically by plotting  $\Delta J_n$  vs.  $\Delta J_t$  for the different temperatures [Arai (1963) in Coe (1967b); see also Figs. 1 and 2]. The data of an ideally behaving sample will form a line whose slope is  $|h|/|h_L|$  from which the paleointensity can be directly determined. The following assumptions are implied by the Thellier method:

- (1) PTRM's acquired in different temperature intervals are independent and additive.
- (2)  $J_n$  is a TRM with negligible secondary components of magnetization.
- (3) Both  $J_n$  and  $J_t$  are in the region where the TRM is linearly dependent on the external field.
- (4)  $J_n$  and  $J_t$  are independent of cooling rates.
- (5) The sample-demagnetizing field due to its surroundings (e.g., the remainder of the lava flow) has a negligible effect on the acquisition of the primary TRM.
- (6) Heating in the laboratory causes no physical or chemical changes of the sample that alter in any way its TRM properties.

Deviations from linearity of the  $\Delta J_n - \Delta J_t$  curves are usually attributed to the failure of one or more of the above assumptions. Effects on the shapes of  $\Delta J_n - \Delta J_t$  plots caused by the violation of some of the above assumptions have been discussed in detail by Coe (1967b, 1973).

Experimentally, it is known that only a small fraction of paleointensity experiments yields reliable results. (It has been said that only rocks which acquire remanence in known magnetic fields yield reliable paleointensities!) Since the Thellier method is so time-consuming and because of the relatively few samples yielding linear  $\Delta J_n - \Delta J_t$  curves over their entire spectrum of blocking temperatures, it is important to understand the causes for non-ideal (non-linear)  $\Delta J_n - \Delta J_t$  curves and the effects of such non-ideal behaviour on paleointensity determinations. It would also be helpful to establish criteria that would help maximize the success of paleointensity determinations. In this paper it will be shown that the presence of MD particles of magnetite causes non-linear

$\Delta J_n - \Delta J_t$  curves; in addition, stability criteria are established to help identify samples which are most likely to exhibit non-linear  $\Delta J_n - \Delta J_t$  curves.

### 3. Description of the magnetite powders

In order to obtain the broadest spectrum of particle-size distributions, both natural and synthetic magnetites were used. The physical descriptions and  $T_C$  values of the magnetite powders and the TRM properties of the corresponding samples are summarized in Table I. The samples and powders are numbered as in Levi (1974).

High-purity natural magnetite crystals whose saturation magnetization,  $J_S(T_R)$ , is  $93 \pm 1$  e.m.u./g and whose Curie point,  $T_C$ , is  $580^\circ\text{C}$  were dry ground and sieved to obtain different size fractions (powders 2–4). Grinding and ball-milling were done in repeated short intervals to avoid heating which might cause oxidation. The X-ray diffraction pattern of one of the ground powders exhibited only spinel lines associated with magnetite, yielding a cubic cell edge of  $8.39 \pm 0.01$  Å.

Synthetic magnetite powders were generously supplied by several sources. Powder 11 (Toda Industries, Japan) is a synthetic magnetite powder whose particles are highly acicular (rod-shaped) with a mean axial ratio of 8 : 1. The expectation that powder 11 contains SD particles is supported by its bulk coercivity.  $H_C = 438 \pm 3$  Oe and by its ratio of saturation remanence to saturation magnetization,  $J_{RS}/J_S = 0.44 \pm 0.01$ . This compares well with the theoretical value,  $J_{RS}/J_S = 0.50$ , for an assemblage of randomly oriented, magnetically uniaxial SD particles. Samples 5–9 contain equidimensional, synthetic magnetite powders, having  $H_C$  values near 100 Oe and  $J_{RS}/J_S$  values of about 0.11. Sample 5 contains magnetite powder supplied by Pfizer Co. (BK-5099); samples 6 and 7 contain identical magnetite powder supplied by the Columbian Carbon Co.; samples 8 and 9 contain identical magnetite powder prepared after a recipe by Elmore (1938).

Electron micrographs were used to determine the particle shapes and size distributions. Depending on the particular powder, between 64 and 249 particles were counted to arrive at the median values. The origins and shapes of the magnetite particles and their

TABLE I  
Physical characteristics of the magnetites and TRM properties of the samples

Sample No.	Particle origin and shape	Particle size, $d$ ( $\mu\text{m}$ )	$T_C$ ( $\pm 10^\circ\text{C}$ ) ( $^\circ\text{C}$ )	TRM ( $H_L = 0.46$ Oe) ( $10^{-3}$ G)	$H_{1/2}$ (Oe)	$T_{1/2}$ ( $^\circ\text{C}$ )	$J/J_L$ liquid $\text{N}_2$ cycles in $h = 0$
2	natural crushed, sieved; irregular	$\bar{d} = 2.7$ $d < 150$	580	0.227	$78 \pm 4$	$475 \pm 15$	0.590 0.465 0.476
3	natural crushed, sieved; irregular	$\bar{d} = 1.5$ $d < 50$	580	2.06	$138 \pm 10$	$493 \pm 10$	0.593 0.521 0.497
4	natural ball-milled; regular polygons	$\bar{d} = 0.31$ $d < 2$	580	0.915	$380 \pm 8$	$444 \pm 10$	0.936 0.888 0.822
5	synthetic regular polygons spheres to cubes	$\bar{d} = 0.24 \pm 0.1$ $d < 0.9$	565	2.87	$347 \pm 5$	$492 \pm 10$	0.945 0.935 0.929
6	synthetic regular polygons spheres to cubes	$\bar{d} = 0.21 \pm 0.06$ $d < 0.5$	570	1.39	$334 \pm 5$	$507 \pm 10$	0.976 0.951 0.965
7	synthetic regular polygons spheres to cubes			13.2	$360 \pm 15$	$508 \pm 10$	0.945 0.961 0.955
8	synthetic regular polygons spheres to cubes	$\bar{d} = 0.12 \pm 0.04$ $d < 0.3$	575	1.08	$292 \pm 10$	$400 \pm 15$	0.990 0.970 0.986
9	synthetic regular polygons spheres to cubes			0.97	$295 \pm 15$	$418 \pm 10$	0.965 0.910 0.907
11	synthetic acicular (needle shape)	mean axial ratio = 8 : 1 $0.35 \times 0.04$	591	3.03	$571 \pm 20$	$519 \pm 10$	1.003 0.995 0.994

$1 \text{ Oe} = 10^{-4} \text{ Wb/m}^2 = 10^{-4} \text{ T}$ .  
 $1 \text{ G} = 1 \text{ e.m.u./cm}^3 = 10^3 \text{ A/m}$ .

median and maximum diameters are listed, respectively, in columns 2 and 3 of Table I.

Synthetic magnetites which are prepared by precipitation from an aqueous solution are usually partly oxidized (Gallagher et al., 1968). In addition, the grinding of the natural magnetite introduces strains into the magnetic particles which substantially influence their magnetic properties. For these reasons and because the Thellier method deals with magnetic behaviour at elevated temperatures, the data of Table I and the bulk magnetic properties discussed above were obtained after heating the magnetite powders to 650°C for 6 h in a slightly reducing environment, using carbon and a residual N<sub>2</sub> atmosphere at pressures of about 10<sup>-1</sup> torr. No higher temperatures were attained in the subsequent experiments. This heat treatment reduced the synthetic powders to stoichiometric magnetite (from X-ray diffraction) and stabilized the powders' magnetic properties through annealing and grain growth (from hysteresis parameters). It is interesting to note that heating to 650°C caused no significant grain growth for particles whose unheated diameters are greater than 0.2 μm (Levi, 1974).

High-field magnetization vs. temperature,  $J-T$ , curves were done for the heated powders; these heatings were also carried out in a similar reducing environment as described above. The curves of all the magnetite powders are reversible within 5%, each exhibiting a single Curie point, listed in column 4 of Table I.

#### 4. Sample preparation and magnetic properties

Samples for the Thellier experiments were prepared by dilutely dispersing a particular magnetite powder in a matrix of high-purity alumina (Alcoa's A-16) and calcium-aluminate cement (Alcoa's CA-25). This matrix has excellent high-temperature characteristics and is non-magnetic for the purposes of the present study (Levi, 1974). The magnetite powder concentration is of the order of 1% by weight, the maximum concentration being less than 4% for sample 3 (due to its low  $J_{RS}/J_S$  value). The sample mixtures were sieved through a 250-μm sieve to break down clumps of the matrix and of the magnetite powder and improve sample homogeneity. The samples were

molded into cylinders about 24 mm in diameter whose height is about 22 mm. Sample volume is usually between 9 and 10 cm<sup>3</sup>, and the samples weigh between 15 and 19 g. The samples were slowly heated to 650°C for 6 h in a slightly reducing environment (identical to the method described in Section 3) to stabilize the chemical and magnetic properties of the samples. The samples were given repeated TRM's, using an identical heating procedure, until the TRM's were reproducible to within 2–3%. All samples spent at least 20 h above 600°C prior to the Thellier experiments of this study.

Some of the samples' pertinent TRM parameters are listed in the last four columns of Table I. Column 5 lists the samples' TRM (1 Gauss = 1 e.m.u./cm<sup>3</sup>) acquired in a laboratory field of 0.46 Oe. These magnetization values are typical of the natural remanence of many igneous rocks. The large difference in the TRM's of samples 6 and 7 is due to approximately an order of magnitude difference in the concentration of their magnetite particles. Differences in the TRM's of other samples are due to both differences in the concentration as well as to intrinsic differences in the magnetites. Column 6 lists the samples' median demagnetizing field,  $MDF \equiv H_{1/2}$ : that peak alternating field required to reduce the sample magnetization to half its initial value. Excluding sample 11, there is a maximum in the MDF data occurring near sample 4, whose mean particle diameter is about 0.31 μm; samples with smaller equidimensional particles have lesser MDF values. The uncertainties associated with the MDF values are deviations from the mean of two independent determinations. Column 7 lists the samples' mean blocking temperatures,  $T_{1/2}$ : that temperature to which the sample must be heated in zero field to demagnetize half its remanence. The remanence is always measured at room temperature. Column 8 gives the samples' TRM-decay after cooling cycles to liquid N<sub>2</sub> temperature and reheating to  $T_R$  in zero field. Temperature cycles to below the isotropic point, which for stoichiometric magnetite is near 130°K (Bickford et al., 1956; Syono and Ishikawa, 1963), were first studied by Ozima et al. (1964). Subsequent studies by Kobayashi et al. (1965) and Merrill (1970) have shown that the relative low-temperature decay of the magnetization decreases with decreasing grain size and is essentially absent for SD particles. It is now known that such low-temperature cycling reduces the remanence in MD particles whose rema-

nence is primarily controlled by magnetocrystalline anisotropy. The data of column 8 is consistent with these findings, showing that the low-temperature decay decreases with grain size from MD to SD particles. The data for each sample represent the fraction of TRM remaining after each of three successive low-temperature cycles. Because the total remanence in magnetite decreases further with each low-temperature cycle, three low-temperature cycles were used to obtain these data. However, the amount of remanence lost in an *individual* cycle usually decreases with each successive cycle such that it is not particularly useful to do more than about three such cycles. It is interesting to note that the pattern of magnetization decay after low-temperature cycles is the one magnetic property which most closely resembles the pattern of the samples' mean particle sizes.

## 5. Experiments and results

In this study of the Thellier method, the sample remanences are always laboratory TRM's (total or partial TRM's) acquired in a constant field of 0.460 Oe. Therefore, assumptions (2)–(5) of the Thellier method (see p. 247), are immediately satisfied. To satisfy assumption (6), to minimize irreversible changes of the samples' TRM properties, the samples' magnetic and chemical properties were first stabilized by heating to 650°C in a slightly reducing chemical environment, as described previously, and an identical procedure was followed for all subsequent heatings of the Thellier experiments. In addition, Levi (in press, 1976) has shown experimentally that the additivity of PTRM's in small external fields,  $h < 0.5$  Oe, is obeyed to the same degree by these samples regardless of their magnetite particle sizes, satisfying assumption (1). Thus the present experiments are designed to test the effect of the magnetite particle size on the Thellier method.

In actual paleointensity determination many parameters which may affect the results are either poorly known or not known at all, such that accuracies of better than 10% are rarely expected or claimed — unless, of course, one is dealing with a sample which acquired remanence in a known field. In the present experiments, however, most of the sample and field parameters are known such that deviations of even

a few percent might be significant.

Modified Thellier experiments were executed following Coe (1967a,b) and Coe and Grommé (1973):

(a) The NRM is measured at  $T_R$ .

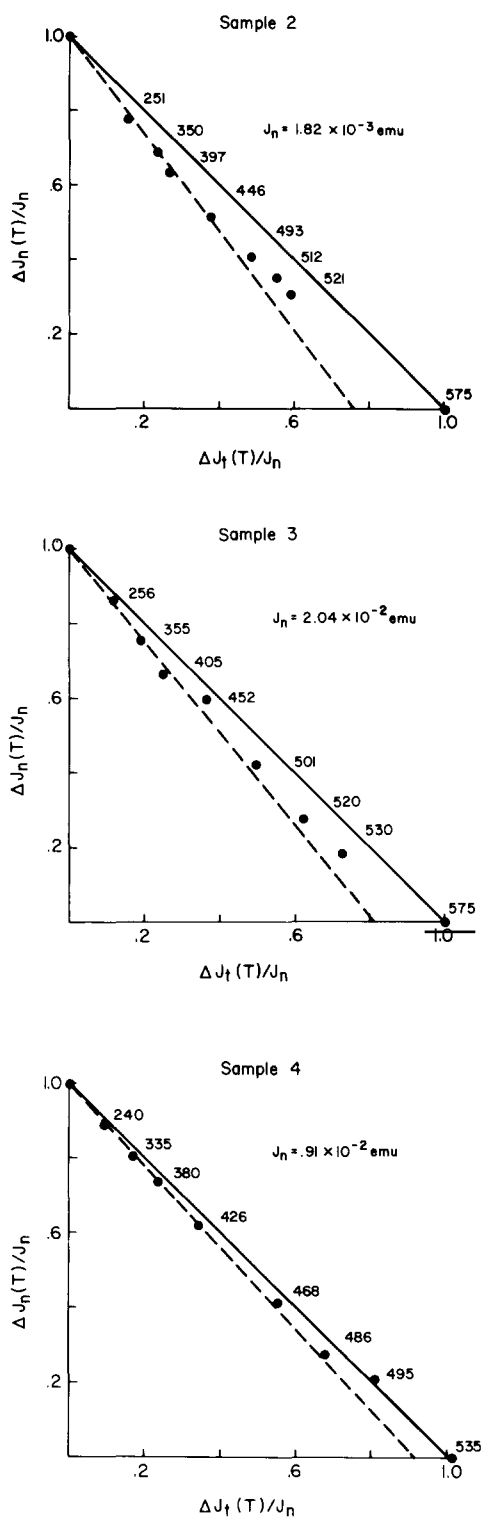
(b) The sample is heated to  $T_1 > T_R$  and cooled back to  $T_R$  in zero field; the magnetization is measured at  $T_R$  to obtain the PNM lost between  $T_R$  and  $T_1$ .

(c) The sample is reheated to  $T_1 > T_R$  and cooled back to  $T_R$  in  $h_L$ . The field  $h_L$  is continuously present throughout the entire heating and cooling cycle. The magnetization is measured at  $T_R$  to obtain the PTRM acquired between  $T_1$  and  $T_R$ .

Steps (b) and (c) are repeated at successively higher temperatures until all the blocking temperatures are exceeded. The temperature is maintained at the particular elevated temperature to allow thermal equilibrium to be established. Depending on the temperature, the time at  $T_1$  varies from 30 to 75 min. The laboratory field,  $h_L$ , in these experiments is known to better than  $\pm 0.5\%$  and is reproducible to within  $\pm 0.5\%$ . The field during step (b) is nulled to within  $\pm 50 \gamma$  in the region of the experiment. The absolute temperature is known to  $\pm 10^\circ\text{C}$ , and the reproducibility of the temperature during a particular step of the paired heatings is determined by an automatic temperature controller and is thought to be better than  $\pm 3^\circ\text{C}$ . The main difficulty encountered in reproducing the temperature is in reproducing the samples' positions in the oven.

The data is represented in Figs. 1 and 2. The magnetization is always normalized with respect to the NRM (laboratory TRM). The remanences are always along the axes of the sample cylinders. The numbers associated with the (PNRM, PTRM) points correspond to the temperature steps in  $^\circ\text{C}$ . The lines are drawn to connect the initial and final points. The initial point is defined as (1.000, 0.000), and the small deviations of the final points from (0.00, 1.00) are attributed to small changes in the samples' TRM upon heating. The lines represent "ideal" behaviour in the Thellier sense.

The points of the  $\Delta J_n - \Delta J_t$  plots for samples 2–4 (Fig. 1) systematically sag below the "ideal" line, and the sag (curvature) decreases from sample 2 to sample 4. A linear approximation to the lower temperature points of samples 2 and 3 results in apparent paleointensities which are systematically high by as much as 35%, depending on the particular number of points used to define the line (Table II). If the linear



approximation is required to include data covering at least half of the sample's magnetization, including data through  $493^{\circ}\text{C}$  for sample 2,  $501^{\circ}\text{C}$  for sample 3 and  $486^{\circ}\text{C}$  for sample 4, the apparent paleointensities, using a least-squares fit, would be systematically high by 22% for sample 2, 14% for sample 3, and 5% for sample 4. These data are in sharp contrast with the ratios of the initial to final points of all three samples which are  $0.99 \pm 0.01$ . The uncertainty represents the deviation from the mean for two determinations for each sample.  $\Delta J_t$  was always parallel to the NRM for samples 2 and 4, and  $\Delta J_t$  was always induced antiparallel to the NRM for sample 3.

It is noteworthy that the deviation from ideal behaviour increases with increasing mean magnetite particle sizes, and with decreasing median demagnetizing field (values for samples 2, 3 and 4 are 78, 138 and 380 Oe, respectively). Both in terms of particle sizes (Table I) and in terms of their stability the magnetic particles of samples 2–4 are typical of those found in many igneous rocks.

The  $\Delta J_n - \Delta J_t$  plots for samples 5–9 and 11 (Fig. 2) are essentially linear for all their blocking temperatures. The reason for the deviation of the  $522^{\circ}\text{C}$  point of sample 6 is not known but may be due to a temperature discrepancy in steps (b) and (c) of the  $522^{\circ}\text{C}$  step of the Thellier experiment. In addition other factors may be involved as some slight reduction is observed for all samples, which is exhibited by the fact that the  $\text{NRM}/\text{TRM} \leq 1$ . In Table III, the slopes of the linear least-squares fits are shown for the  $\Delta J_n - \Delta J_t$  data of samples 5–9 and 11. Although the value for sample 6 is  $-0.89$ , by excluding the  $522^{\circ}\text{C}$  point the least-squares slopes becomes indistinguishable ( $-0.96$ ) from the ratios of the initial to final points. Samples 8 and 9 contain the same magnetite powder and their TRM properties are quite similar. In the Thellier experiments sample 8 was always given PTRM's antiparallel to the NRM, and for sample 9 the PTRM's were given parallel to the original NRM; despite these differences in procedure, both samples are seen to have nearly identical

Fig. 1. Normalized  $\Delta J_n - \Delta J_t$  curves for samples 2–4. Solid lines represent ideal behaviour in the Thellier sense. Broken lines are linear approximations of the lower-temperature data. The numbers associated with the points are the temperatures in  $^{\circ}\text{C}$  of the heating steps.

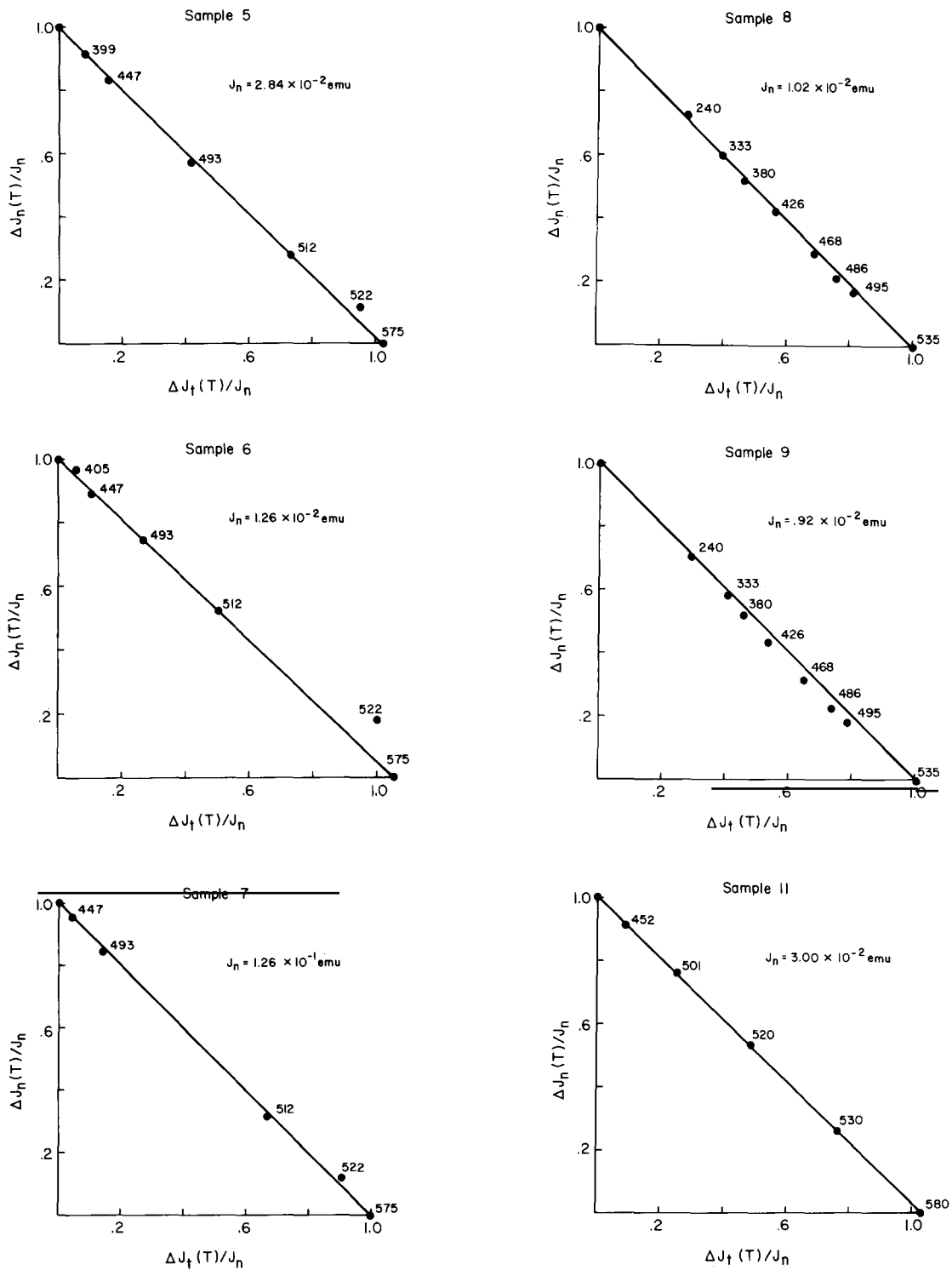


Fig. 2. Normalized  $\Delta J_n - \Delta J_t$  curves for samples 5-9 and 11. Solid lines join the initial and final points. The numbers associated with the points are the temperatures in  $^{\circ}\text{C}$  of the heating steps.



TABLE II

Linear least-squares fit of  $\Delta J_n - \Delta J_t$  data for MD samples

Sample 2			Sample 3			Sample 4		
$T$ ( $^{\circ}\text{C}$ )	$J/J_n$	slope of line	$T$ ( $^{\circ}\text{C}$ )	$J/J_n$	slope of line	$T$ ( $^{\circ}\text{C}$ )	$J/J_n$	slope of line
397	0.63	-1.36	405	0.67	-1.34	380	0.74	-1.10
446	0.57	-1.30	452	0.60	-1.15	426	0.62	-1.09
493	0.41	-1.22	501	0.42	-1.14	468	0.41	-1.05
521	0.31	-1.14	530	0.18	-1.12	486	0.28	-1.05
Ratio of end-points		-0.99 $\pm$ 0.01			-0.99 $\pm$ 0.01			-0.99 $\pm$ 0.01

$\Delta J_n - \Delta J_t$  plots. The data for sample 11 indicate very linear behaviour, which is comforting, since sample 11 contains needle-shaped single-domain particles.

For completeness it should be stated that samples 1 and 10 do exist but were not included in this article. Sample 1 is a chip (3.569 g) from a single crystal of stoichiometric magnetite, which has such unstable remanence that no meaningful  $\Delta J_n - \Delta J_t$  curve can be constructed. In contrast, sample 10 is very stable and the corresponding  $\Delta J_n - \Delta J_t$  curve is linear throughout the entire spectrum of blocking temperatures; the data for sample 10 are omitted, because, due to the very dilute concentration of the magnetite particles, their sizes and shapes are not known.

In the Thellier experiments described thus far the procedure of Coe (1967a,b) was followed; this method is different from that described by Thellier and

Thellier (1959). To see whether the experimental results depend on the particular procedure, the experiments were repeated following the procedure of Thellier and Thellier, where the samples are always heated in presence of the laboratory field, as outlined below.

(a) The NRM is measured at  $T_R$ .

(b) The sample is heated to  $T_1 > T_R$  and cooled back to  $T_R$  in the continuous presence of  $h_L$ ; the magnetization is measured at  $T_R$ .

(c) The sample is rotated  $180^{\circ}$  about a horizontal axis normal to the laboratory geomagnetic meridian.

(d) The sample is reheated to the same  $T_1 > T_R$  and cooled back to  $T_R$  in the continuous presence of  $h_L$ . The magnetization is measured at  $T_R$ .

Half the vector sum of the remanences measured after steps (b) and (d) represents the PNM that would remain after heating to temperature  $T_1$  in zero field. Half the vector difference of the remanences obtained in steps (b) and (d) represents the PTRM acquired between  $T_1$  and  $T_R$ . Steps (b), (c) and (d) are repeated at successively higher temperatures until all the blocking temperatures are exceeded. The data obtained using the Thellier procedure (Levi, 1974) has the same features as the data obtained using Coe's procedure of Figs. 1 and 2:

(i) The  $\Delta J_n - \Delta J_t$  plots of samples 2-4 sag below the line connecting the initial and final points and are concave up with respect to it.

(ii) The  $\Delta J_n - \Delta J_t$  plots of samples 5-9 and 11 are essentially linear, and as in the previous runs the  $\Delta J_n - \Delta J_t$  plots of samples 8 and 9 sag somewhat below the line connecting the initial and final points.

TABLE III

Linear least-squares fit of  $\Delta J_n - \Delta J_t$  data for SD and PSD samples (all points)

Sample	Slope of linear least-squares fit (all points)	Ratio of initial to final points
5	-0.95	-0.98 $\pm$ 0.01
6	-0.89	-0.96 $\pm$ 0.01
7	-0.98	-1.00
8	-1.02	-1.00
9	-1.01	-1.00
11	-0.96	-0.96

## 6. Explanation of the non-linear $\Delta J_n - \Delta J_t$ curves

Since the non-linear  $\Delta J_n - \Delta J_t$  curves are observed only for samples containing MD particles and because the non-linearity increases with an increasing fraction of MD particles, it is concluded that the observed non-linear  $\Delta J_n - \Delta J_t$  curves are indeed due to the presence of MD remanence carrying particles. To explain the non-linear behaviour the following observations must be explained: (1) The non-linear  $\Delta J_n - \Delta J_t$  curves are always concave-up; (2) the same concave-up non-linear behaviour is observed when the PTRM is produced both parallel and antiparallel to the original remanence; and (3) the same type of non-linear curves is observed for both the Thelliers' (1959) and Coe's (1967a,b) executions of the Thellier experiment.

Only a very simplified model for MD remanence is considered, which is essentially identical to the one discussed by Schmidt (1973) consisting of rectangular particles of width  $a$  and length  $2a$ , whose two domains are separated by a single  $180^\circ$  domain wall. It is assumed that the same domain configuration is maintained for all temperatures  $T < T_C$ . Temperature variations of the domain-wall width ( $\delta$ ) are neglected, and it is assumed that  $\delta/a \ll 1$ . Any external field ( $h$ ) is applied in the plane of the domain wall, whose area  $S = a^2$ . In their demagnetized state each particle consists of two oppositely magnetized domains of equal size. The coordinate  $x$  is defined to measure the displacement of the wall from its demagnetized position such that the particle magnetization ( $J$ ) is given by:

$$J = (x/a)J_S$$

where  $J_S$  is the saturation magnetization. To discuss the remanence of such particles an energy function is constructed, assuming that the particles do not interact. Following Schmidt (1973), the following magnetic interactions are considered:

(a) The magnetostatic energy due to the interaction of the particle magnetization ( $J$ ) and the external field ( $h$ ) is:

$$U_M = -\mathbf{h} \cdot \mathbf{JV} = -2AJ_S hx$$

(b) The magnetostatic self-energy of the interaction of the particle magnetization and the demagnetizing field ( $H_d$ ) due to the surface poles is:

$$U_D = -\frac{1}{2} H_d \cdot \mathbf{JV} = (DJ_S^2 A/a)x^2$$

$D$  is the particle demagnetizing factor, which is dependent on the particle geometry and domain configuration, and, although it is a gross oversimplification,  $D$  is assumed to be a constant.

(c) The third energy term is due to the interaction of the domain wall with stress accumulations in the particle caused by crystal imperfections and the presence of impurities. The distribution of stress concentrations is given by  $F(r)$  which is assumed to be temperature independent. The interaction is strongly affected by  $J_S$ , according to the relation  $J_S^P$ , where  $P$  is an exponent  $>2$ . An additional temperature dependence is present in the value for the stress ( $\sigma$ ) which usually decreases with increasing  $T$ :

$$U_W = -CJ_S^P \sigma(T)F(r)$$

where  $C$  is a measure of the interaction at  $T = 0^\circ \text{K}$ .

The energy equation becomes:

$$U = -2AJ_S hx + (DAJ_S^2/a)x^2 - CJ_S^P \sigma(T)F(r) \quad (3)$$

The temperature dependence of the energy function is contained in  $J_S$  and in  $\sigma$ , and because of the varying temperature dependence of the different energy factors, the effects on the remanence of the different energy terms become dominant at different temperatures. Just below  $T_C$ ,  $U_M$  is dominant, and it exerts pressure on the domain wall:

$$p_M = \frac{-\partial U}{A \partial x} = 2J_S h$$

favouring homogeneous particle magnetization, thus tending to force the wall out of the particle. At lower temperatures, as  $J_S$  increases, the wall experiences increasing pressure due to the grain self-demagnetizing energy trying to displace the wall to a more demagnetized position in the interior of the particle.  $U_W$  also increases with decreasing temperature, expressing the increase in the interaction of the domain wall with the particle's stress field, which produces barriers to the domain-wall movement. TRM is blocked at temperature  $T_B$ , when the wall can no longer overcome such an energy barrier. Although at  $T_B$  the wall may have barely been blocked (i.e., wall movement at  $T_B$  might have been blocked near the top of a particular energy barrier) as the temperature decreases below  $T_B$ , the energy barriers increase faster than the other energy terms, because of the greater temperature dependence of  $U_W$  such that near room temperature ( $T_R$ ) the wall

finds itself blocked by a formidable barrier.

With decreasing temperature  $U_D$  increases more rapidly than  $U_M$ ; at  $T < T_B$  there is net demagnetizing pressure on the wall, favouring a new wall position, which should yield a more demagnetized particle. This is equivalent to saying that for  $T < T_B$  the wall climbs part way up the potential-energy barrier, but since  $U_W$  increases more rapidly than both  $U_M$  and  $U_D$  the wall remains blocked. When the field is removed at  $T_R$ , as for measuring the remanence, the net negative pressure on the domain wall is greater yet, so that in the absence of stress accumulations,  $J = 0$  would be the equilibrium state for the particle's magnetization. However, the wall is blocked and there is no change in the remanence.

As the particle is reheated to  $T_B$  in zero field,  $J_S$  decreases affecting a decrease of the energy barriers. The absence of an external field during the thermal demagnetization step, places the particle in a higher energy configuration than during the blocking of the original TRM. Equivalently, the absence of an external field produces a net negative pressure acting on the domain wall. The presence of thermal fluctuations implies that there is a finite probability that sufficient energy will be available for the domain wall to overcome its potential-energy barrier. The mechanism by which this energy becomes available is not known, but it is probably related to the probability of generation of spin waves with the required energy. When sufficient energy is available for the domain wall to overcome the energy barrier, the self-demagnetizing pressure:

$$p_D = -2[DSJ_S^2/a]x$$

will drive the wall toward the particle's demagnetized configuration. (During the acquisition of the original TRM the availability of sufficient energy to overcome the barrier will result in no net demagnetization, because at  $T_B$  and in the presence of  $h$  there is no net pressure on the domain wall.)

During the PTRM step the particle is reheated to  $T_B$  in the presence of an external field. The domain wall is subjected to a magnetizing pressure:

$$p = 2J_S h - 2[DJ_S^2]x$$

which drives the wall to the demagnetized side of the "blocking" potential barrier. Due to the presence of the external field during the PTRM step, the input of

slightly more energy than during the thermal demagnetization is required for the wall to overcome the barrier. In addition, the magnitude of the outward (magnetizing) pressure on the wall during the PTRM step is less than the demagnetizing pressure during the thermal demagnetization step. Thus a two-domain particle which is thermally demagnetized by heating to a particular temperature  $T_1$  is likely to be remagnetized with less remanence when reheated to  $T_1$  in an external field of equal intensity to the original TRM-producing field. This model requires higher temperature or more intense field during the PTRM step to produce  $\Delta J_t = \Delta J_n$ . In terms of viscous remanence, the above model predicts that at a given temperature the spontaneous decay of TRM is greater than the viscous acquisition in an external field equal to the TRM field. This conclusion is identical to that of Dunlop (1973b, pp. 873–879), regarding the viscous magnetization of two-domain particles.

For the MD model discussed above the PNRM lost during thermal demagnetization of a total TRM between  $T_R$  and some temperature  $T_1 < T_C$  exceeds the PTRM acquired by cooling from  $T_1$  to  $T_R$  in an external field of equal intensity to the field which imparted the original TRM. For an ensemble of MD particles with distributed blocking temperatures, this would lead to the concave-up  $\Delta J_n - \Delta J_t$  curves that are observed for samples containing MD particles. Since the particles which are critical in the discussion of the above model are statistically demagnetized after the thermal demagnetization step, the same behaviour is expected whether the PTRM is induced parallel to antiparallel to the original remanence. Concave-up  $\Delta J_n - \Delta J_t$  curves are predicted for both the Thelliers' (1959) and Coe's (1967a,b) executions of the Thellier method. It is predicted that the degree of curvature of the  $\Delta J_n - \Delta J_t$  curves will increase for increasing fractions of MD remanence. Generalizing the above model to include more complex MD particles would seem to explain the observed concave-up  $\Delta J_n - \Delta J_t$  curves of samples 2–4, and it should apply equally well to MD particles of all ferri- and ferromagnetic substances. Clearly, this mechanism is valid only for MD particles. Therefore, the linear  $\Delta J_n - \Delta J_t$  curves of samples 5–9 suggest that for equidimensional magnetite particles with diameters less than  $0.25 \mu\text{m}$  the acquisition of TRM and its thermal demagnetization are not through domain-wall movements.

## 7. Discussion

We have seen that samples containing SD magnetite particles (sample 11) and samples containing small particles, which are entirely in the submicron size range (samples 5–9) behave ideally in the Thellier sense. In addition, linear  $\Delta J_n - \Delta J_t$  plots of the magnetite samples correlate with high stabilities with respect to alternating fields, AF ( $H_{1/2} \gtrsim 300$  Oe). This has also been observed by Kono (1974) for volcanic rocks. On the other hand, there is no apparent relationship between blocking temperatures,  $T_{1/2}$ , and the degree of linearity of the PNRM–PTRM curves. There is high correlation between linear PNRM–PTRM curves and high magnetization resistance to temperature cycles in zero field to below magnetite's isotropic temperature. Such low-temperature cycles in magnetites provide a measure for the fraction of the remanence residing in non-SD sized particles. Comparison of columns 8 and 3 of Table I shows that the low-temperature cycles provide a better measure than AF or thermal stability for the relative magnetite grain sizes of the samples. More than 50% of the TRM of samples 2 and 3 decays after three successive low-temperature cycles, but there is less than 10% decay of the TRM of samples whose magnetite particles are wholly submicron. The behaviour of sample 4 is particularly interesting because of its high AF stability,  $H_{1/2} = 380$  Oe (second only to sample 11), although 18% of its remanence decays after three low-temperature cycles. The concave-up  $\Delta J_n - \Delta J_t$  curve for sample 4 suggests that for magnetites the low-temperature decay character is more reliable than AF stability as a predictor for ideal behaviour in a Thellier experiment.

Whenever non-linearities in the  $\Delta J_n - \Delta J_t$  curves are observed during a Thellier experiment, it is common to calculate the ancient field intensity from a linear approximation to the lower-temperature data, the rationale being that physical and chemical changes that irreversibly alter the sample's TRM properties are much more likely at elevated temperatures. This has been recently demonstrated by Coe and Grommé (1973). The experiments discussed here show that whenever multidomain particles contribute to a sample's TRM, non-linear PNRM–PTRM curves may result, which are concave-up with respect to the "ideal" line, and this behaviour is not associated with

irreversible changes of the sample. Rather, it is due to intrinsic, reproducible differences between the remanence of MD particles on the one hand and SD and submicron magnetite particles on the other, and to the lack of symmetry of the domain-wall movements during the two heatings of the Thellier experiment.

A linear approximation to the lower-temperature data of samples 2–4 would lead to substantial errors in the paleointensity, which would always lead to paleointensities which are higher than the actual field, although the ratio of the end-points gives the correct results. On the other hand, if only the higher blocking-temperature data are used, the analysis would lead to apparent paleointensities lower than the actual field. Similar behaviour was observed by Coe (1967a,b) for the 1915 A.D. Mount Lassen dacite. Coe speculated at that time that the curious behaviour was due to the presence of multidomain particles.

It has been amply demonstrated that high temperatures can and often do cause irreversible changes in a sample's TRM properties, thus it is *not* advocated that the NRM/TRM ratio be used for paleointensity determinations. Such a procedure would discard the consistency checks for which the Thellier method was originally developed. Conversely, the experiments discussed here show that non-linear PNRM–PTRM diagrams cannot be assumed to be caused by irreversible changes of the TRM properties of the sample. If the geomagnetic intensity is to be determined using non-linear PNRM–PTRM diagrams, further experiments must be conducted to determine the cause of the non-linearity. For example, the PTRM test proposed by Thellier and Thellier (1959) can be used to redetermine PTRM acquisition at lower temperatures. Changes in the PTRM show that irreversible changes have taken place. However, Coe (1967b) pointed out that the Thelliers' PTRM test cannot detect irreversible changes of magnetic regions with blocking temperatures higher than the PTRM intervals; thus reproducibility of PTRM is a necessary but not sufficient condition to prove that no irreversible changes have occurred in the sample's TRM properties. A further test to check whether observed non-linearities are intrinsic to the sample's magnetic properties or whether they are due to irreversible changes of the sample is to repeat the Thellier experiment, using as "NRM" a laboratory TRM. If the same or similar non-linear features are observed in both Thellier experiments,

and if the end-points of the P'NRM'–PTRM curve reproduce the laboratory field, then the linear approximation to the lower temperature data might lead to an erroneous paleointensity. The NRM/TRM ratio should not be used by itself for paleointensity determinations, unless further tests justify its use.

If tests show that a sample's TRM properties undergo irreversible changes at higher temperatures, then an intensity determination, using a linear approximation to the lower-temperature data might yield a reliable result, provided the samples' NRM's are characterized by high AF stabilities,  $H_{1/2} \gtrsim 300$  Oe. The last statement is very subjective and depends on the accuracy desired for the paleointensity determination and on the fraction of the NRM used to obtain the linear approximation. For a particular accuracy, lesser stabilities would require that a relatively greater fraction of the NRM be used and conversely; see Table II. Sample 4 couples non-linear behaviour with high AF stability of its TRM. However, using 60% of the NRM for a linear approximation, the resulting error in the intensity is only 5%, which is an acceptable error for most experiments. For magnetites and titanomagnetites that exhibit a low-temperature magnetocrystalline anisotropy transition [less than 10% ulvöspinel, according to Syono (1965)] a better stability test to assess the potential linearity of the PNRM–PTRM curves is the stability of the magnetization subject to temperature cycles to below the isotropic point. In magnetites, TRM decay of less than 10% is an indication for linear PNRM–PTRM curves.

As a consequence of the above discussion, it might be prudent to re-assess existing paleointensity data with particular emphasis on cases where a linear approximation to the lower-temperature points is used without sufficient justification in determining paleointensities.

In the preceding discussion we have been preoccupied with linear  $\Delta J_n - \Delta J_t$  curves. If the framework outlined by the assumptions of the Thellier method is satisfied and if the resulting Thellier experiment yields a linear  $\Delta J_n - \Delta J_t$  curve for the sample's entire blocking-temperature spectrum, then the geomagnetic intensity is obtained directly from the slope of the line. However, a linear  $\Delta J_n - \Delta J_t$  plot in itself, is a necessary but not sufficient condition for a reliable and accurate intensity determination. It is easy to visualize a post-igneous process whereby assumption (2) (p. 247) is violated through recrystallization or

oxidation and unmixing of the magnetic minerals. Such a change might be subtle and difficult to detect and the resulting magnetization (no longer the original TRM) might be stable, yielding  $\Delta J_n - \Delta J_t$  curves that are linear, whose slope is totally unrelated to the paleofield.

## 8. Conclusions

The Thellier method for paleointensity determinations has been applied to prepared samples containing magnetite whose mean particle sizes range from SD to MD. The following are the principal findings.

(1) Linear (ideal)  $\Delta J_n - \Delta J_t$  curves are obtained for samples containing SD and submicron magnetite particles.

(2) There is positive correlation between linear  $\Delta J_n - \Delta J_t$  curves and high stability of the magnetization: (1) with respect to AF demagnetization,  $H_{1/2} \gtrsim 300$  Oe; and (2) with respect to temperature cycles in zero field to below magnetite's isotropic temperature,  $J/J_t > 0.90$ .

(3) When a large fraction of the remanence resides in MD particles, non-linear (concave-up)  $\Delta J_n - \Delta J_t$  curves are observed such that a linear approximation to the lower blocking-temperature data leads to apparent paleointensities that are higher than the actual paleofield; however, the ratio of the end-points, NRM/TRM, yields the correct (laboratory) intensity.

(4) The non-linear (non-ideal)  $\Delta J_n - \Delta J_t$  curves, associated with MD particles, are explained in terms of the lack of symmetry of the domain-wall movements during the two heatings of the Thellier experiment.

(5) Paleointensity determinations should be based on data spanning the sample's entire blocking-temperature spectrum, and, whenever non-ideal behaviour is observed, further tests should be conducted to determine whether the non-linear behaviour is caused by irreversible physical or chemical changes of the sample or whether the non-linear behaviour is intrinsic to the magnetic particles.

(6) If non-linearities are caused by irreversible changes of a magnetite containing sample, an accurate paleointensity might be obtained from a linear approximation of the unaltered lower-temperature data, provided the sample is characterized by high AF sta-

bility,  $H_{1/2} \gtrsim 300$  Oe, and high stability with respect to temperature cycles in zero field to below the isotropic point,  $J/J_t > 0.90$ .

(7) Paleointensities should not be obtained solely from the ratio NRM/TRM, because such a procedure would forfeit the built-in consistency checks for which the Thellier method was so painstakingly developed.

### Acknowledgements

I would like to thank Professor Ronald T. Merrill for his encouragement, many valuable discussions and for his helpful suggestions and criticisms of this manuscript. I have benefited substantially from discussions with Professor Minoru Ozima, especially in regard to mechanisms explaining the observed non-linear  $\Delta J_n - \Delta J_t$  curves. I would also like to thank Professors S.K. Banerjee and P.N. Shive for their helpful comments on this paper. Funding was provided by National Science Foundation grants (GA-27570, DES 72-01 541-A01 and DES 75-14800).

### References

- Bickford, L.R., Brownlow, J.M. and Penoyer, R.F., 1956. Magnetocrystalline anisotropy in cobalt substituted magnetite single crystals. *Proc. Inst. Electr. Eng., Part B*, 104: 238–244.
- Butler, R.F. Banerjee, S.K., 1975. Theoretical single-domain grain-size range in magnetite and titanomagnetite. *J. Geophys. Res.*, 80: 4049–4058.
- Carmichael, C.M., 1967. An outline of the intensity of the paleomagnetic field of the Earth. *Earth Planet. Sci. Lett.*, 3: 351–354.
- Coe, R.S., 1967a. Paleointensities of the Earth's magnetic field determined from Tertiary and Quaternary rocks. *J. Geophys. Res.*, 72: 3247–3262.
- Coe, R.S., 1967b. The determination of paleointensities of the Earth's magnetic field with special emphasis on mechanisms which could cause nonideal behavior in Thelliers' method. *J. Geomagn. Geoelectr.*, 19: 157–179.
- Coe, R.S., 1973. Effects of shape anisotropy paleointensity determinations. *EOS (Trans. Am. Geophys. Union)*, 54: 1072 (abstract).
- Coe, R.S. and Grommé, C.S., 1973. A comparison of three methods of determining geomagnetic paleointensities. *J. Geomagn. Geoelectr.*, 24: 415–435.
- Dunlop, D.J. 1973a. Thermoremanent magnetization in sub-microscopic magnetite. *J. Geophys. Res.*, 78: 7602–7613.
- Dunlop, D.J., 1973b. Theory of magnetic viscosity of lunar and terrestrial rocks. *Rev. Geophys. Space Phys.*, 11: 855–901.
- Elmore, W.C., 1938. Ferromagnetic colloid for studying magnetic structures. *Phys. Rev.*, 54: 309–310.
- Evans, M.E., 1972. Single-domain particles and TRM in rocks. *Comments Earth Sci. Geophys.*, 2: 139–148.
- Evans, M.E. and Wayman, M.L., 1970. An investigation of small magnetic particles by means of electron microscopy. *Earth Planet. Sci. Lett.*, 9: 365–370.
- Folgheraiter, M., 1899. Sur les variations séculaires de l'inclinaison magnétique dans l'antiquité. *J. Phys. (Paris)*, 8: 660–667.
- Gallagher, K.J., Feitknecht, W. and Mannweiler, U., 1968. Mechanism of oxidation of magnetite to  $\gamma\text{-Fe}_2\text{O}_3$ . *Nature (London)*, 217: 1181–1121.
- Kobayashi, K., Campbell, M.F. and Moorhead, J.B., 1965. Size dependence of low-temperature change in remanent magnetization of  $\text{Fe}_3\text{O}_4$ . 1965 Annu. Proc. Rep. Rock Magn. Res. Group Jpn., pp. 33–50.
- Kono, M., 1974. Intensities of the Earth's magnetic field about 60 m.y. ago determined from the Deccan trap basalts, India. *J. Geophys. Res.*, 79: 1135–1141.
- Levi, S., 1974. Some magnetic properties of magnetite as a function of grain size and their implications for paleomagnetism. Ph.D. Thesis, University of Washington, Seattle, Wash., 210 pp.
- Merrill, R.T., 1970. Low-temperature treatments of magnetite and magnetite-bearing rocks. *J. Geophys. Res.*, 75: 3343–3349.
- Morrish, A.H. and Yu, S.P., 1955. Dependence of the coercive force on the density of some iron oxide powders. *J. Appl. Phys.*, 26: 1049–1055.
- Ozima, M., Ozima, M. and Akimoto, S., 1964. Low temperature characteristics of remanent magnetization of magnetite. *J. Geomagn. Geoelectr. Jpn.*, 16: 165–177.
- Parry, L.G., 1965. Magnetic properties of dispersed magnetite powders. *Philos. Mag.*, 11: 302–312.
- Rimbert, F., 1959. Contribution à l'étude de l'action de champs alternatifs sur les aimantations rémanentes des roches, applications géophysiques. *Rev. Inst. Fr. Pét.*, 14: 17–54 and 123–155.
- Roquet, J., 1954. Sur les rémanences des oxydes de fer et leur intérêt en géomagnétisme. *Ann. Géophys.*, 10: 226–247 and 282–325.
- Schmidt, V.A., 1973. A multidomain model of thermoremanence. *Earth Planet. Sci. Lett.*, 20: 440–446.
- Shaw, J., 1974. A new method of determining the magnitude of the paleomagnetic field. *Geophys. J.R. Astron. Soc.*, 39: 133–141.
- Soffel, H., 1971. The single domain–multidomain transition in natural intermediate titanomagnetites. *Z. Geophys.*, 37: 451–470.
- Syono, Y., 1965. Magnetocrystalline anisotropy and magnetostriction of  $\text{Fe}_3\text{O}_4\text{-Fe}_2\text{TiO}_4$  series with special application to rock magnetism. *Jpn. J. Geophys.*, 4: 71–143.
- Syono, Y. and Ishikawa, Y., 1963a. Magnetocrystalline aniso-

- tropy of  $x\text{Fe}_2\text{TiO}_4 \cdot (1-x)\text{Fe}_3\text{O}_4$ . *J. Geomagn. Geoelectr.*, 18: 1230–1231.
- Thellier, E., 1938. Sur l'aimantation des terres cuites et ses applications géophysiques. *Ann. Inst. Phys. Globe, Paris*, 16: 157–302.
- Thellier, E. and Thellier, O., 1959. Sur l'intensité du champ magnétique terrestre dans le passé historique et géologique. *Ann. Géophys.*, 15: 285–376.
- Van Zijl, J.S.V., Graham, K.W.T. and Hales, A.L., 1962. The paleomagnetism of the Stormberg lavas of South Africa, 1 and 2. *Geophys. J.R. Astron. Soc.*, 7: 23–39 and 169–182.
- Wilson, R.L., 1961. Paleomagnetism in northern Ireland, Part 1: The thermal demagnetization of natural magnetic moments in rocks. *Geophys. J.R. Astron. Soc.*, 5: 45–58.